EL SEVIER

Contents lists available at ScienceDirect

Thin Solid Films

journal homepage: www.elsevier.com/locate/tsf



Structure and AC conductivity of nanocrystalline Yttrium oxide thin films

V.H. Mudavakkat ^a, M. Noor-A-Alam ^a, K. Kamala Bharathi ^a, S. AlFaify ^b, A. Dissanayake ^b, A. Kayani ^b, C.V. Ramana ^{a,*}

- ^a Department of Mechanical Engineering, University of Texas at El Paso, El Paso, TX 79968, USA
- ^b Department of Physics, Western Michigan University, Kalamazoo, MI 49008, USA

ARTICLE INFO

Article history:
Received 13 December 2010
Received in revised form 25 April 2011
Accepted 27 April 2011
Available online 6 May 2011

Keywords:
Yttrium oxide
Thin films
Crystal structure
Structural transformations
Composition
Rutherford backscattering spectroscopy
Electronic transport
Relaxation

ABSTRACT

Yttrium oxide (Y_2O_3) thin films were grown at substrate temperatures (T_s) ranging from room temperature (RT) to 500 °C and their structural and electrical properties were evaluated. The results indicate that Y_2O_3 films grown at RT-100 °C were amorphous $(a-Y_2O_3)$. Y_2O_3 films began to show cubic phase $(c-Y_2O_3)$ at $T_s = 200$ °C. The average grain size varies from 5 to 40 nm as a function of T_s . Room temperature ac electrical conductivity increases from $0.4~(\Omega-m)^{-1}$ to $1.2~(\Omega-m)^{-1}$ with increasing T_s from RT to 500 °C. The frequency dispersion of the electrical resistivity reveals the hopping conduction mechanism. Frequency dispersion of the electrical resistivity fits to the modified Debye's function, which considers more than one ion contributing to the relaxation process. The mean relaxation time decreases from 2.8 to $1.4~\mu s$ with increasing T_s indicating that the effect of microstructure of the Y_2O_3 films is significant on the electrical properties.

© 2011 Elsevier B.V. All rights reserved.

1. Introduction

Yttrium oxide (Y₂O₃) received significant attention in recent years by the scientific and research community mainly due to the potential application of the material in various technological fields. Y₂O₃ exhibits excellent electronic and optical properties such as transparency over a broad spectral range (0.2–8 µm) [1–3], high dielectric constant (14–18) [1–6], high refractive index (\sim 2) [3], large band gap (5.8 eV) [3,4], low absorption in the broad spectral range (from near-UV to IR) [5,6], superior electrical break-down (>3 MV/cm) [1–6]. In addition, low leakage current onto silicon substrates, lattice match with Si and ease to be doped with rare earth ions makes Y2O3 interesting for integrated electronics and optoelectronics applications [1–6]. As the ionic radius of Y^{3+} is close to those of rare earths, Y_2O_3 is also largely investigated as a rare earth doped host material for being used as optical amplifiers, photo-and cathodoluminescent phosphors [7–9]. Structurally, Y₂O₃ is a c-type rare-earth oxide [10,11]. The c-type structure of Y_2O_3 is stable up to 2325 °C in air [10,11]. The c-type structure is a modified fluorite-type cubic structure with one fourth of the anion sites vacant and regularly arranged. AC conductivity of Y₂O₃ arises due to the hopping of electrons between the Y^{3+} ions connected via the oxygen ions $(Y^{3+}-0-Y^{3+})$. In addition, the AC conductivity depends on the number of grains and grain boundaries. Therefore, understanding the microstructure-dependent ac conductivity is very important in order to tune the conditions to produce Y_2O_3 films for the desired electronic device applications. Specifically, fundamental understanding of the electrical properties is important for employing Y_2O_3 films in gate dielectric and storage capacitors for dynamic random access memories [3–5,7,12].

The controlled growth and manipulation of the microstructure of Y₂O₃ films, at the nanoscale dimensions, has important implications for the design and applications of Y₂O₃ films. Furthermore, the ability to tailor the properties so as to optimize performance requires a detailed understanding of the relationship between electronic and geometric structure, particularly at the nanoscale dimensions. In this context, the present work was performed on the growth and electrical characterization of nanocrystalline Y2O3 films made by magnetron sputterdeposition. Frequency-dependent conductivity, which is a major part of this work apart from structural characterization, is an important analytical method to study the electrical properties, conduction mechanism and the dispersion of relaxation times of Y₂O₃ films. Interestingly, we found that there exists a correlation between the microstructure and electrical properties, specifically the grain-size dependent electrical conductivity and their dispersion profiles. The results obtained are presented and discussed in detail in this paper.

2. Experiments

2.1. Fabrication

Y₂O₃ films were deposited onto silicon (Si) (100) wafers by radiofrequency magnetron sputtering. The experimental conditions

^{*} Corresponding author. Tel.: +1 915 747 8690; fax: +1 915 747 5019. E-mail address: rvchintalapalle@utep.edu (C.V. Ramana).

employed for Y₂O₃ film fabrication are listed in Table 1. The Si (100) substrates were cleaned by a procedure as reported elsewhere [13,14]. Thoroughly cleaned and dried substrates were introduced into the vacuum chamber, which was eventually evacuated to a base pressure of $\sim 1.33 \times 10^{-4}$ Pa. Yttrium (Y) metal target (Plasmaterials Inc.) of 2 in. diameter and 99.95% purity was employed for reactive sputtering. The Y-target was placed on a 2 in. sputter gun, which is placed at a distance of 8 cm from the substrate. The flow of the Ar and O₂ and their ratio was controlled using a mass flow meter. Before each deposition, the Y-target was pre-sputtered for 10 min using Ar alone with shutter above the gun closed. The deposition was carried out with a sputtering power of 100 W to obtain ~55 nm thick films. The samples were deposited at different temperatures (Ts) varying from room temperature (RT) to 500 °C. The substrates were heated by halogen lamps and the desired temperature was controlled by Athena X25 controller.

2.2. Characterization

 Y_2O_3 films were characterized by performing structural and electrical measurements. X-ray diffraction (XRD) measurements were performed by using a Bruker D8 Advance X-ray diffractometer. All the measurements were made ex-situ as a function of growth temperature. XRD patterns were recorded using Cu K α radiation (λ = 1.54056) at RT. The coherently diffracting domain size (D_{hkl}) was calculated from the integral width of the diffraction lines using the well known Scherrer's equation after background subtraction and correction for instrumental broadening. The Scherrer equation is [15]:

$$D_{hkl} = \frac{0.9\lambda}{\beta cos\theta} \tag{1}$$

where D_{hkl} is the size, λ is the wavelength for the anode material used in the XRD machine, β is the width of a peak at half of its intensity, and θ is the angle of the peak. Ion beam analysis of the samples was performed using the 6 MV tandem accelerator. Rutherford backscattering spectra (RBS) were recorded using a 2.0 MeV beam of He⁺⁺ ions with a 0° angle of incidence measured from the sample normal. Backscattered ions were collected using a silicon surface barrier detector at a scattering angle of 165° the sample normal. Composition profiles were determined by comparing SIMNRA computer simulations of the spectra with the original data [16]. Frequency dependant conductivity measurements were carried out employing a LCR meter (HP 4192A). The measurements were made at room temperature by varying the applied ac frequency to obtain the dispersion profiles.

3. Results and discussion

The XRD patterns of Y_2O_3 films are shown in Fig. 1. The patterns are shown as a function of T_s . The XRD curve (Fig. 1) of Y_2O_3 films grown at T_s = RT–100 °C did not show any peaks indicating their characteristic amorphous (a- Y_2O_3) nature. The XRD peak (JCPDS 43–613) corresponding to cubic phase (c- Y_2O_3) began to appear for Y_2O_3 samples grown at T_s = 200 °C. However, the peak (at ~29°) is rather

Table 1 Sputtering deposition conditions employed for Y₂O₃ films.

Deposition parameter	Set value
Base pressure Sputtering pressure	~0.13 mPa ~0.13 Pa
Target	Y-metal (5 cm×0.32 cm)
Substrates	Si(100)
Substrate temperature (T_s)	RT-500 °C
Target-substrate distance	8 cm
RF power	100 W
Film thickness	~55 nm

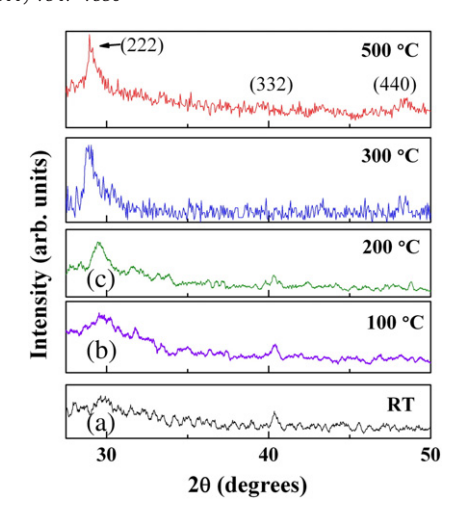


Fig. 1. XRD patterns of Y_2O_3 films grown at various substrate temperatures. Y_2O_3 films grown at RT and 100 °C exhibit the amorphous nature. Increasing temperature results in the formation of cubic structure of Y_2O_3 films.

broad. It is evident (Fig. 1) that the intensity of the peak, which corresponds to diffraction from (222) planes, increases with increasing T_s . This is an indicative of an increase in the average grain-size with increasing T_s . The crystallite size D_{hkl} calculated using the Scherrer equation is found to be in the range of 5–40 nm for Y_2O_3 films grown in the range of $T=200-500\,^{\circ}$ C. The (440) peak began to appear at $T_s \ge 300\,^{\circ}$ C. The appearance of specific diffraction peaks indicates that the growth process initiates with (111) planes due to the lowest surface energy [1]. With increasing T_s , the in-plane organization of the structure and random oriented nano-grains results in the appearance other characteristic peaks. Most important to note is the diffuse nature of XRD curves, in spite of the appearance of (222) peak, indicating the nano-crystallites embedded in the amorphous matrix.

Chemical compositional analyses using RBS measurements indicated the growth of compositionally stoichiometric Y₂O₃ films in the substrate temperature range of 200–500 °C. Fig. 2 shows the experimental Rutherford backscattering (RBS) spectrum of an Y₂O₃ film grown at 200 °C (circles) along with the simulation curve (lines) calculated using SIMNRA code. The simulated curve was calculated using SIMNRA code [16] for the fixed set of experimental parameters: (1) incident He⁺ ion energy, (2) integrated charge, (3) energy resolution of the detector, and (4) scattering geometry. The backscattered ions observed were due to various elements, and the positions are indicated by arrows for the experimental spectrum. The scattering

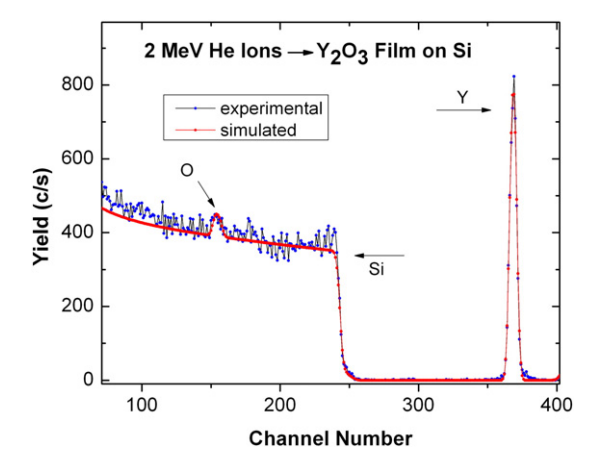


Fig. 2. RBS spectra of Y_2O_3 films grown at $T_s = 200$ °C. The experimental (circles) and simulated (line) RBS curves are shown. Excellent agreement between the experimental and calculated curves can be noted.

Download English Version:

https://daneshyari.com/en/article/1667807

Download Persian Version:

https://daneshyari.com/article/1667807

<u>Daneshyari.com</u>